LA-UR 94-3468

Los Alamos National Laboratory is operated by the University of California for the United States Department of Energy under contract W-7405-ENG-36

TITLE HEAVY ION COLLISIONS

AUTHOR(S). Barbara V. Jacak, P-25

SUBMITTED TO: Presented at International Conference on High Energy Physics, Glasgow, Scotland, July, 1994

DISCLAIMER

Los Alamos Los Alamos National Laboratory
Los Alamos, New Mexico 87545

FORM NO R1F 114
ST NO 2629 5/81

HEAVY ION COLLISIONS

Barbara V. Jacak*

Los Alamos National Laboratory
Los Alamos, New Mexico 87545, USA

Abstract

Heavy ion collisions at very high energies provide an opportunity to recreate in the laboratory the conditions which existed very early in the universe, just after the big bang. We prepare matter at very high energy density and search for evidence that the quarks and gluons are deconfined. I describe the kinds of observables that are experimentally accessible to characterize the system and to search for evidence of new physics. A wealth of information is now available from CERN and BNL heavy ion experiments. I discuss recent results on two particle correlations, strangeness production, and dilepton and direct photon distributions.

1. Introduction

High energy heavy ion collisions provide the opportunity to create hadronic matter at high energy density in the laboratory, and study its properties. I will discuss the motivation for these studies and the methods employed. Numerous results from experiments at 14.6 GeV/nucleon at the Brookhaven AGS, and at 200 GeV/nucleon at the CERN SPS have become available over the last several years. These experiments have measured a number of observables to characterize the system prepared, and to look for evidence of new physics occurring in these collisions. Instead of describing all of the measurements, I will focus on three areas of recent interest and summarize new results that were shown at this conference. These areas include characterization of the collision using Bose-Einstein correlations, strangeness production, and dilepton and direct photon production.

Figure 1 shows the phase diagram of hadronic matter, plotted as a function of temperature and baryon density. At low temperature and modest baryon density ($\rho/\rho_0 = 1$) the realm of normal nuclear matter is found. The study of the phase transition of this matter, which can be quite well described as a liquid, to a nucleon and pion gas is the subject of heavy ion collisions at intermediate energy. The shaded region indicates the temperature and baryon density range expected for the phase transition from a hadron gas to a quark-gluon plasma in which the quarks become deconfined. This transion along with chiral symmetry restoration, which

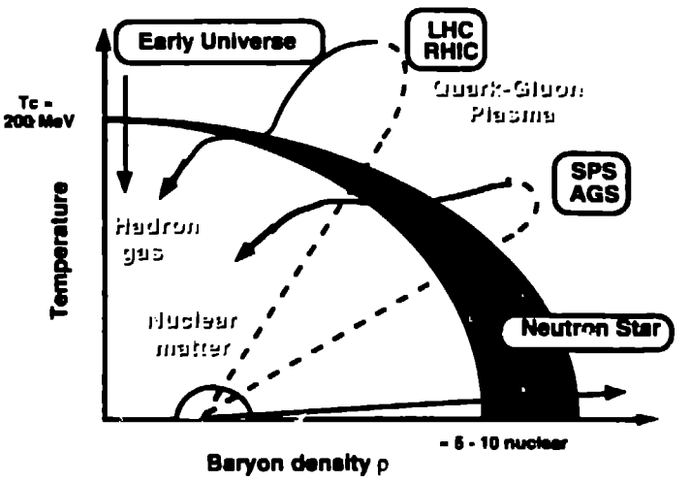

Figure 1. Phase diagram of hadronic matter.

* E-mail: jacak@lanl.gov

occurs under similar conditions, are predicted by the standard model.[1] Calculations of QCD on the lattice [2] indicate a critical temperature near 150 MeV. There is currently considerable discussion as to the order of the phase transition. It is expected to be second order; even if it is first order, the finite system size and particle number (not to mention short lifetime of the system) are expected to smear the discontinuities in a first order transition.[2,3,4]

The paths followed through the phase diagram by the early universe, at low baryon density, and a forming neutron star, at low temperature, are indicated on the figure. Also shown are two possible paths followed by heavy ion collisions, which aim to create quark matter in the laboratory by increasing both the temperature and the baryon density. Of course, the hot compressed matter does not live very long in these collisions before expanding and cooling back to normal hadronic matter, and it is not at all certain that either thermal or chemical equilibrium is reached.

We address these issues experimentally by measuring various particles emitted at different times in the evolution of the collision. Though they are produced over the entire space-time evolution of the collision, leptons and photons are emitted most copiously from the hottest, highest energy density zone reflect the temperature of the early system. They are unaffected by the surrounding hadronic matter as they interact only electromagnetically. Unfortunately, these probes are rare and difficult to measure, and are plagued with large backgrounds from the hadronic phase. Kaons and pions are emitted later, at the time of "freeeout" when the hadrons cease to interact. Their correlations provide a picture of the space-time evolution of the later part of the collision. The relative rates of kaon, pion baryon and anti-baryon production may provide an indication of the approach to chemical equilibrium.

It should be noted that nuclear matter in its ground state has an energy density of approximately 0.17 GeV/fm^3, while the energy density inside a nucleon is about four times this. The phase transition to quark matter is predicted to occur at an energy density near 2-3 GeV/fm^3.[1] We study such systems in the laboratory with heavy ions to achieve maximum energy density over as large a volume as possible. This should maximize the time available to approach equilibrium and enhance signals of interesting physics over the background. However, it is possible that quark matter may already be produced in p-p collisions, so systematic studies of p-p, p-nucleus and nucleus-nucleus collisions are required.

2. OBSERVABLES

In characterizing the collisions, we would like to ascertain the size and density of the hot system in the central region of the nucleus-nucleus system and determine the energy density achieved. It is important to know how well the nuclei stop each other to see how much longitudinal energy is converted to transverse energy, and what baryon density exists in the central region. Furthermore, we need to determine whether or not the system approaches equilibrium and thermodynamic descriptions may be used. The tools available to address these questions include two-particle correlations to map the space-time extent of the system when the hadrons decouple.[5] The flow of energy and charged particles transverse to the beam along with the rapidity distribution of protons indicate the amount of stopping and randomization of the incoming energy. The transverse mass distributions of hadrons reflect the temperature of the system at freezeout and effects of radial expansion.[6] The production ratios of different particles are related to the extent of chemical equilibrium reached in the collision and subsequent evolution of the hadron gas.

Having used these observables to ascertain that we have prepared a system of sufficient energy density and spatial extent in which it is reasonable to look for evidence of a phase transition to a new type of matter, we turn to a second class of observables. These reflect the high energy density region and provide potential signals of deconfinement and/or chiral symmetry restoration.

The widths and branching ratios of vector mesons depend strongly on the matter surrounding the meson when it decays.[7,8] The ϕ meson mass and width are modified if chiral symmetry is restored.[9]. The ϕ decay is very sensitive to modification of the kaon mass by chiral symmetry restoration as its mass is very near that of two kaons. The decay ratio $\phi \rightarrow K^+K^-/\phi \rightarrow e^+e^-$ may be quite different than in vacuum.[10] The ϕ meson is readily measurable, even in high multiplicity events, due to its narrow peak structure. Decays of the ρ and ω can be used to measure the lifetime and temperature of the hot hadron gas before freezeout.[8]

Some of the predicted signals of deconfinement are suppression of J/ψ production by Debye screening of $c\bar{c}$ in a quark-gluon plama,[11] or enhanced production of strange-[12] and anti-quarks[13] along with hadrons containing them. Large fluctuations in the charged particle multiplicity or transverse energy distribution could arise from bubbles of decaying plasma.[14] In addition to characterizing the collision, two particle correlations can signal a phase transition as they measure the duration of hadronization and particle emission, which should be long in both a first or second

order phase transition.[5] In very high energy collisions, as at the planned heavy ion colliders, we may look for quenching of jets, indicating plasma formation by the larger dE/dx in plasma than in hadronic matter.[15] Also, it has been predicted that charm production may be significantly enhanced in a quark-gluon plasma.[16]

3. BOSE-EINSTEIN CORRELATIONS

As mentioned above, the measurement of two-particle correlation functions, and analysis of the Bose-Einstein correlations is of great interest as it yields the space-time evolution of the hadronic (i.e. later) part of the collision. The lifetime and transverse expansion may be strongly influenced by the phase transition. The measured correlation function represents the Fourier transform of the particle distribution inside the emitting source if 1) the particles are emitted incoherently, 2) they do not come from resonance decays, 3) the particles do not interact with each other or the rest of the system, and 4) there are no kinematic correlations. Correlation functions are customarily fit assuming a Gaussian distributed source, though it is known that the assumptions above are not completely correct and the distribution has a more complex shape.[17,18] High statistics data allow multi-dimensional fits. These do not require the unrealistic assumption of a spherical source, are more sensitive to the collision dynamics, and less influenced by relativistic effects than correlations analyzed in the four-momentum difference (q_{inv}) of the two particles which represents an average over all directions of the pairs within the acceptance of the experiment.

The experimental correlation functions are constructed from the ratio of the two-particle cross section to the product of the two single particle cross sections, evaluated by taking particles from different events. These are usually fit with the function:

$$C_2 = C(q_{t_o}, q_{t_s}, q_l) = D[1+\lambda exp[(-q_{t_o}^2 R_{t_o}^2 - q_{t_s}^2 R_{t_s}^2 - q_l^2 R_l^2)]$$

The relative momentum vector is decomposed into a longitudinal component, q_l, parallel to the beam axis, and two transverse components, q_{t_o} and q_{t_s}, which are perpendicular to the beam axis. q_{t_o} is along the momentum sum of the two particles, and q_{t_s} is perpendicular to it. Being parallel to the velocities of the particles, q_{t_o} is sensitive to the lifetime of the source,[5] and $R_{t_o}^2 = R_{t_s}^2 + (\beta\Delta\tau)^2$. The R parameters are related to the Gaussian sizes of the source in the specified directions; the correspondence of the R parameters and the sizes is discussed below. The strength of the correlation is given by the λ parameter, sometimes called the chaoticity parameter.

Different experiments analyze correlations in somewhat different reference frames. NA44[19,20] analyzes

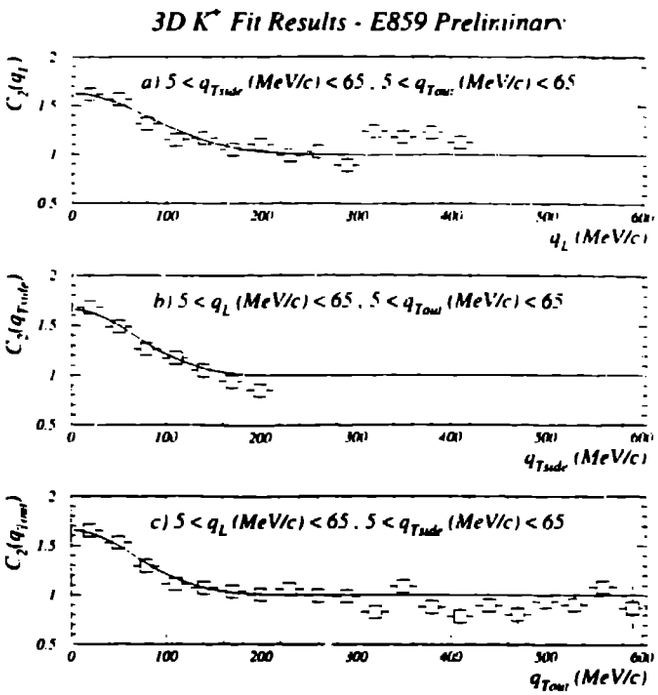

Figure 2. K^+K^+ Correlation functions from 14.6 GeV/nucleon Si + Au collisions.

in the frame in which the particle pair momentum sum along the beam direction is zero. This frame couples the lifetime information solely to q_{t_o}. NA35[21,22] and E802/E859[23,24] analyze in the nucleon-nucleon center of mass frame, which is similar (but not identical) near mid-rapidity. This reference frame is near the rest frame of the particle source.

Figure 2 shows the correlation function of K^+ pairs in 14.6 GeV/nucleon Si + Au collisions, measured by E859[25] and analyzed in three dimensions as described above. The projection in each direction is shown; cuts are made on small momentum differences in the other two directions. The solid line shows a fit with a Gaussian source distribution; the shape of the data is reproduced quite well. The E859 extracted radius, or R, parameters are shown in Table 1. The transverse radius parameters from kaons are smaller than those from pions, and the λ parameter is larger. Both trends are expected from the fact that fewer kaons than pions are produced by the decays of long-lived resonances. Such decay products are formed after freezeout, and represent an uncorrelated background to the Bose-Einstein signal, hence the decrease in the λ parameter. Resonances with lifetimes comparable to, but somewhat longer than, the source lifetime modify the shape of the correlation function and tend to increase the magnitude of the extracted R parameters. Within statistical errors, R_{t_o}

pair	R_l	R_{t_s}	R_{t_o}	λ
$\pi^+\pi^+$	2.75±0.15	2.95±0.19	2.77±0.13	0.65±0.02
K^+K^+	1.71±0.14	2.09±0.20	2.07±0.16	0.83±0.08

Table 1. E859 correlation function fit parameters

and R_{t_o} are the same.

NA35 is a streamer chamber and TPC experiment at CERN, with a large acceptance for pions from 200 GeV/nucleon S - nucleus collisions. They have studied the correlations and resulting fit parameters as a function of rapidity and transverse momentum. NA35 finds[21] the rapidity dependence of the transverse radius parameters to be minimal, and of R_l to indicate a longitudinal expansion very similar to the boost-invariant expansion which was predicted for these energies.[26] The transverse radius parameters decrease somewhat with increasing p_t.

Both NA35[21] and NA44,[19,20] which measures π and K correlations in 200 GeV/nucleon S + Pb, find no evidence for a long-lived pion emission; as at the lower energy, $R_{t_s} \approx R_{t_o}$. Figure 3 shows R_{t_s} extracted by NA44 for both pions and kaons, as a function of m_t. The dashed line and squares indicate $2/\sqrt{m_t}$, and agree with the data remarkably well.[20] This dependence on $\sqrt{m_t}$ is notable because a simple hydrodynamical model of a cylindrically symmetric expanding source predicts just such a dependence.[27] The common behavior with m_t of pions and kaons suggests equilibration and supports the applicability of hydrodynamics. The expansion creates correlations between a particle's position and momentum, negating one of the assumptions made in fitting correlation functions and relating the fit parameters to the source size. In the hydrodynamical picture, the fit parameters reflect the velocity gradient and freezeout temperature.[27] I will come back to this point below, as it affects how we may use the extracted R parameters.

A tool to guide interpretation of the correlation fit parameters is comparison with an event generator incorporating the collision dynamics, particle production, hadron rescattering, and resonance formation and decay. Many experiments currently use the RQMD event generator[28], which gives good agreement with single particle distributions. To study correlation functions, the model is used to generate the phase-space coordinates of hadrons at the time they suffer their last strong interaction. Using the freezeout position and momentum of pairs of randomly selected particles, a two-particle symmetrized wave function is calculated and used to add Bose-Einstein correlations.[17,18] The particles are first subjected to the experimental acceptance cuts, and the resulting correlation functions are then fit in the same way as the data.

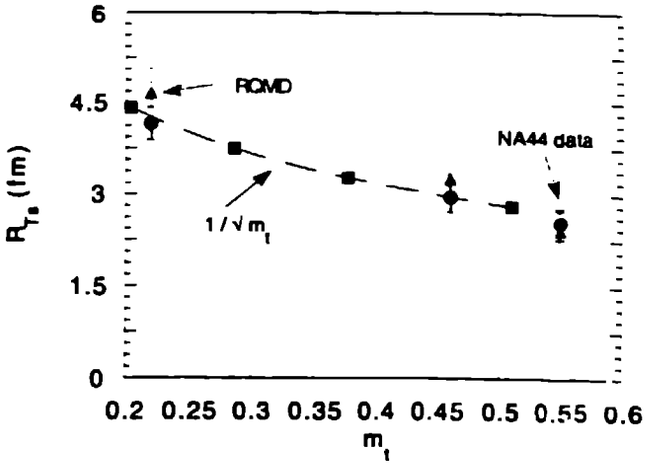

Figure 3. m_t dependence of R_{t_s} parameters from NA44 and RQMD for 200 GeV/nucleon S + Pb. The dashed line and squares show $1/\sqrt{m_t}$, scaled to the data.

NA44 and NA35 both find good agreement of the RQMD correlation functions with the data; Figure 3 shows the fit parameters from RQMD events along with the NA44 data. RQMD clearly has the same $\sqrt{m_t}$ dependence as the data. We can then look into the details of the collisions in the model to understand this trend. RQMD does show a radial expansion of the source, which is driven by multiple secondary collisions among the many produced hadrons before freezeout.[20] This agrees with the conclusions drawn from the simple hydrodynamical model above. This expansion causes a difference between the extracted R parameters and the actual size of the source at freezeout. The RQMD comparisons also explain the differences in the fit parameters between different experiments; these arise due to the different acceptances in y and p_t. It is interesting to note that at lower energy, experiment E814 also finds good agreement between measured pion correlation functions and those predicted by RQMD.[29] They also use the RQMD comparison to infer evidence of expansion of the source before freezeout.

The event generator comparison provides a way to determine the relationship between the correlation fit parameters and the source size we wish to measure. This can be accomplished by comparing the calculated correlation function with the particle distributions at freezeout. Such a comparison is shown in Figure 4 for S + Pb collisions at 200 GeV/nucleon.[18]

The top half of Figure 4 shows the pion (solid lines) and kaon (dotted lines) distributions at freezeout along the beam direction, transverse to the beam, and in time. The fact that the kaon distributions are narrower than the pions is clearly visible, and this trend agrees with the data. The lower section of the figure shows

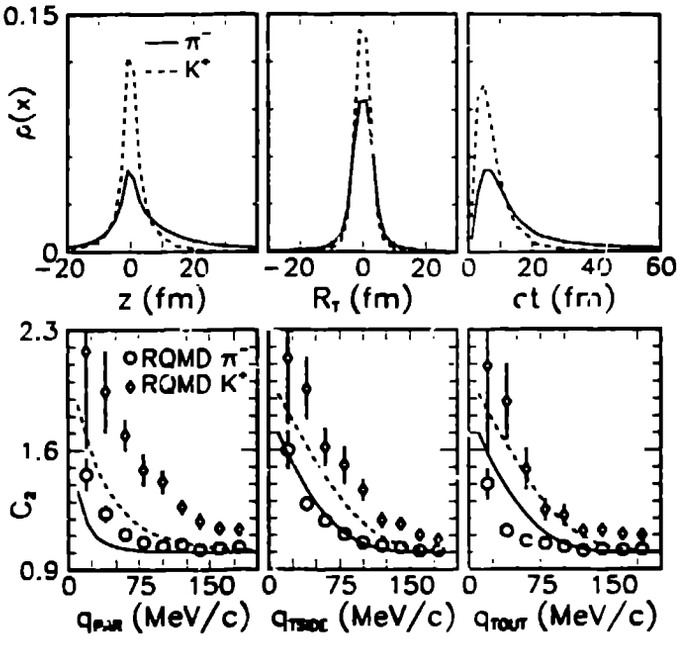

Figure 4. Position distributions (top) and correlation functions (bottom) at freezeout for π and K pairs from RQMD 200 GeV/nucleon S + Pb collisions. Both are shown in three dimensions.

correlation functions calculated several ways from the RQMD events. They are plotted in the variable which correspond most closely to the directions in the top part of the figure, along the beam direction (q_{par} or q_l), transverse to the beam (q_{tside}), and in q_{tout}, which is a combination of the time and transverse size. The solid and dashed lines indicate the Fourier transform of the position distributions in the top part of the figure. The points show the calculated RQMD correlation functions using the NA35 experimental acceptance. Comparison of the curves allows evaluation of how closely the correlation functions measured by the experiments actually reflect the source sizes. It is evident that the agreement is far from perfect. Along the beam direction, there are significant effects of Lorentz extention of the measurement reference frame with respect to the source frame,[30] along with the position-momentum correlations caused by the longitudinal expansion.[27,21] Analysis in q_{t_o} most closely approximates the transverse size of the source, but is also subject to error from position-momentum correlations induced by transverse expansion. This correlation increases with increasing particle transverse mass, and is reflected in the larger deviation of the calculated correlation function from the kaon Fourier transform. The position-momentum correlation increases the difference between K and π fit parameters, and causes the m_t dependence shown in Figure 3. The correlation functions in q_{t_o} should not agree directly with the time distribution as they also include the source transverse size. These effects can be untangled, however, by using the information from the event generator to scale the R parameters extracted from the data.

The recent high statistics experiments and careful event generator comparisons have shown that Bose-Einstein correlations reflect the collision dynamics in addition to providing information about the source size and shape at the time of freezeout. Interpretation of the fit parameters to correlation functions is complicated, however. They do not directly yield the source size. It is possible, however, to extract the information by using an event generator, comparing to data, and then looking at the event generator position distributions.[18,19,29].

4. STRANGENESS PRODUCTION

A number of experiments at both BNL and CERN have searched for evidence of enhanced production of particles incorporating strange quarks. Such an enhancement is a possible signal of deconfinement as the large mass of the strange quark does not greatly suppress $s\bar{s}$ production at the temperatures expected for transition to a quark-gluon plasma. The time needed for saturation of the strange phase space in the plasma through gluon fusion is only a few fm/c, whereas the rate for strange pair production in conventional hadronic processes is much slower.[12,31] (Multi)strange antibaryon production is particularly sensitive as these are difficult to produce in hadronic interactions and are unlikely to reach equilibrium amounts in a hadron gas.[32] Strange particle production can also yield information on the evolution of the hadronic stage of the collisions, and the approach to chemical equilbrium.[31]

Enhanced production of K^+ was observed at 14.6 GeV/nucleon by E802.[33] The hadronic environment in the central region at that energy is rather baryon-rich, and the K^+ enhancement can be understood quantitatively via the associated production mechanism $\pi + N \rightarrow K^+ + \Lambda$.[34] At 200 GeV/nucleon, enhanced K^+ production was also observed, but in the target region rather than at midrapidity.[35] It should be noted that at $y \approx 1$ in 200 GeV/nucleon S + W, the baryon rapidity density is the same as in midrapidity Si + Au at 14.6 GeV/nucleon. The K^+/π ratios measured by the two experiments are also the same, yielding experimental support for the associated production explanation of the observed K^+ enhancement. Furthermore, enhanced Λ production was seen at target rapidity by NA35 in asymmetric nucleus-nucleus collisions and in p-nucleus collisions.[36] This further supports the associated production explanation.

Enhanced production of antilambdas at midrapidity has been observed by NA35[36], NA36[37] and

particle	ratio A-A	ratio p-p
$\overline{\Lambda}/\Lambda$	0.23 ± 0.01	
$\overline{\Xi}/\Xi$	0.51 ± 0.06	
Ξ^-/Λ	0.094 ± 0.007	
$\overline{\Xi}^-/\overline{\Lambda}$	0.22 ± 0.02	0.06 ± 0.02
$(\Omega^- + \overline{\Omega}^-)/(\Xi^- + \overline{\Xi}^-)$	0.8 ± 0.4	
$(\Omega^- + \overline{\Omega}^-)/(\Xi^- + \overline{\Xi}^-)$	>0.4 (95% C.L.)	<0.15 (90% C.L.)

Table 2. Strange baryon and antibaryon production ratios

WA85[38]. There is an ongoing debate as to whether this enhancement can be explained by the superposition of nucleon-nucleon collisions and secondary particle rescattering, or if new physical processes are required. For example, the RQMD event generator cannot reproduce the $\overline{\Lambda}$ yield without collective excitation of overlapping strings.[39]

Recent measurements of Ξ by WA85 and NA36[38, 37] and Ω by WA94[40] also indicate enhanced strangeness production, compared to p-p collisions. The measured particle ratios in the range $2.5 < y < 3.0$ and $1.2 < p_t < 3.0$ GeV/c are given in Table 2.[38, 41] The ratio $\overline{\Xi}^-/\overline{\Lambda}$ measured by WA85 in sulfur induced collisions is ≈ 5 times greater than that in p-p[41]. The observed enhancement of multistrange antibaryons has not been successfully described by any model incorporating only known physics, and has caused considerable interest in further experimental and theoretical study.

5. DILEPTONS AND PHOTONS

As mentioned above, leptons and photons are produced during the whole lifetime of the collision, but the high energy part of the thermal spectrum is dominated by the hottest, highest energy density region. Its temperature determines the slope of the transverse energy distribution of real and virtual photons, and the emission rate reflects the parton density in this region. The dependence of the photon rate on charged particle multiplicity (i.e. linear or quadratic) aids in identifying the source of photons or dileptons; parton or hadron annihilation produces photons (real or virtual) proportionally to the square of the multiplicity. Experimentally, the production rate and shape of the dilepton mass and p_t spectra are compared to a superposition of hadronic decays in p-p collisions and to p-nucleus measurements. Anomalies can indicate the importance of new physics.

I will discuss the lepton pair results starting at low then moving to higher mass. The mass spectrum separates into regions in which dilepton production is dominated by different processes, though of course, various hadron decays contribute a large fraction of the observed dileptons. The soft continuum region, below the the ρ, should arise predominantly from pion annihilation[42] or thermal emission.[43,44] The mass region around 1 GeV/c^2 includes dileptons from decays of ρ, ω and ϕ mesons, which can yield information about strangeness enhancement, chiral symmetry restoration, and the lifetime of the hot hadron gas. The intermediate mass continuum, between the ϕ and the J/ψ, should be composed predominantly of leptons from decays of open charm, low mass Drell-Yan production, and perhaps the tail of the thermal dilepton distribution. The J/ψ production rate is of interest due to predictions of suppression by quark-gluon plasma. Furthermore, the rate and p_t distribution are affected by initial and final state scattering effects and probe the comoving matter.[45] The high mass continuum above the J/ψ arises primarily from the Drell-Yan process at CERN SPS energy.

In the soft continuum region there has long been an unexplained excess, referred to as "anomalous lepton pairs".[46] The HELIOS I experiment was optimized to study electron and muon pairs from the π through the ϕ, and has recently reported results from 450 GeV p-Be collisions.[47] HELIOS was able to reconstruct the η and ω Dalitz decays, and consequently to properly account for their contributions to the soft dilepton spectrum, previous estimates used too small a value for $\sigma_\eta/(\sigma_\rho + \sigma_\omega)$. Incorporating the η Dalitz rate observed by HELIOS in estimating the soft dileptons from hadronic sources explains the measured spectrum very well, leaving no room for anomalous pairs.[47] Above the π^0, the soft continuum is dominated by η Dalitz decays up to a mass of 0.5 GeV/c. $\omega \rightarrow e^+e^-\pi^0$ then dominates until the ρ, ω peak.

The soft continuum region has recently been investigated in 450 GeV p-Be and p-Au, and 200 GeV/nucleon S-Au collisions by the CERES collaboration.[48] The experiment uses Ring Imaging Cherenkov detectors to track and identify electron pairs at midrapidity with minimal sensitivity to the copiously produced pions. Figure 5[48] shows the mass spectrum of dielectrons from the three systems, compared to the yield expected in the CERES acceptance from known (hadronic) sources. The p_t and pair angle cuts used in the data analysis are indicated on the plots; the higher charged particle multiplicity causes more background in S-Au and requires the larger p_t cut than in proton-induced collisions. The shaded band indicates the dielectron spectrum expected from known sources, filtered through the CERES acceptance and smeared for the experimental resolution and efficiencies. The curves for p-Au and S-Au collisions are calculated by scaling the p-Be prediction by the observed charged particle multiplicity in the dielectron rapidity region. The agreement with the

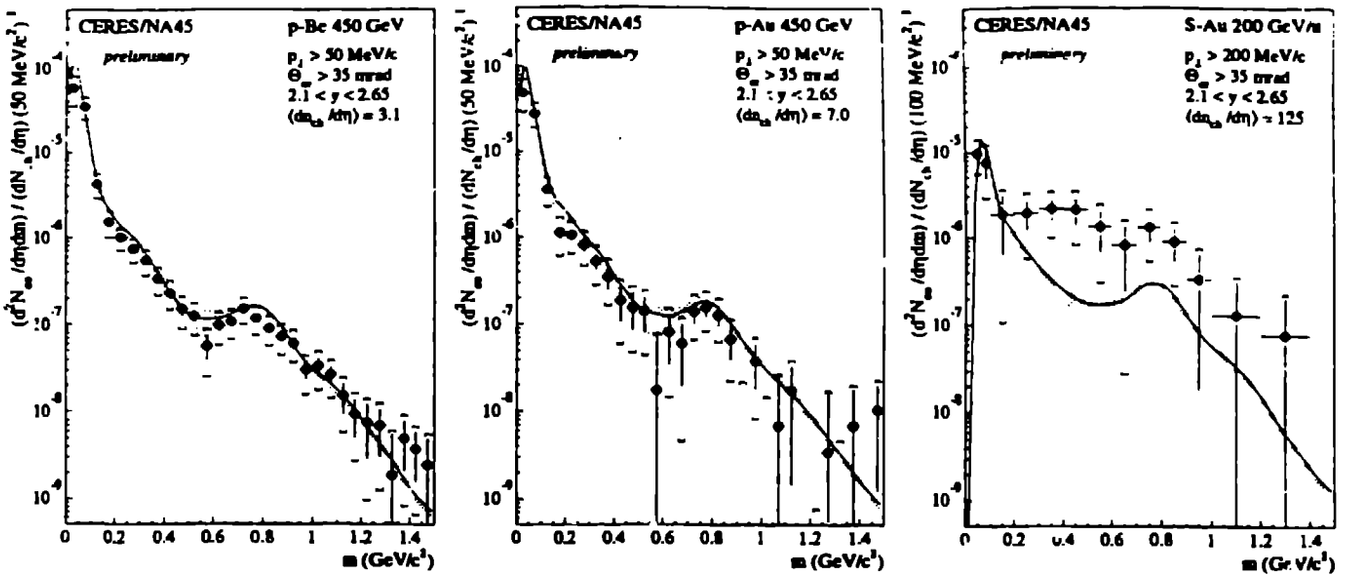

Figure 5. Inclusive mass spectra of e^+e^- pairs in p-Be, p-Au and S-Au collisions measured by CERES. The data are normalized to give pair density per charged particle density within the CERES y acceptance. No pair-acceptance corrections are applied.

data for p-Be and p-Au collisions is very good, but the known sources significantly underpredict the S-Au dielectron yield below the ρ. The magnitude of the enhancement is is a factor of 4.96 ± 0.73 (stat) +1.95/-2.1 (syst).[48] The onset of the enhancement at pair masses above approximately 250 MeV/c^2 suggests it might arise from the opening of the two-pion annihilation channel at $m = 2m_\pi$.

Excess production of dileptons in the soft continuum region was also observed by HELIOS/3,[49] which compares dimuon production in 200 GeV/nucleon S-W collisions with 450 GeV p-W collisions. Figure 6 shows the dimuon mass spectrum for both systems at $y \approx 4$; the curves show the dimuon rate normalized to the number of charged particles at the same rapidity. The S-W curve lies above the p-W curve in the soft region, labeled "LMR" for low mass region, and also in the intermediate mass region, "IMR". The magnitude of the soft excess in HELIOS/3 is qualitatively comparable to that reported by CERES, though the rapidity regions differ somewhat. The intermediate mass excess is 1.96 ± 0.58 above the p-W rate per charged particle.[49] The NA38 collaboration has also observed excess dimuon production in the intermediate mass region, and reports an enhancement of 1.4 ± 0.1.[50]

These enhancements are currently not well understood. It has been suggested that the intermediate mass excess may arise from larger charm production in heavy ion collisions than expected by scaling p-p or p-nucleus collisions.[49,50] However, it is possible that part of the

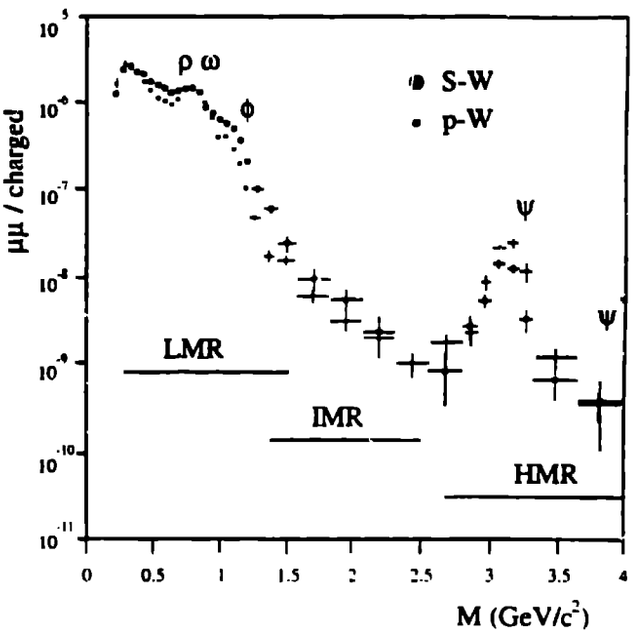

Figure 6. Dimuon mass spectrum measured by HELIOS/3 in S-W and p-W collisions at 200 GeV/A and 450 GeV, respectively. The data are normalized to the charged particle multiplicity.

enhancements in Figures 5 and 6 may appear because of the way that the expected dilepton yield is scaled for comparison to heavy ion data. All three experiments scale dilepton production from hadronic sources by the

charged particle multiplicity - CERES and NA38 scale the Monte Carlo predictions for p-p collisions, and ME-LIOS/3 scales p-W data as well as the predicted yield. It certainly makes sense to scale hadronic sources with the number of hadrons, but it should be noted that the A dependence of charm production in p-nucleus collisions is not quite the same as the A dependence of charged particle production. Charm production scales with a larger exponent in A^α than soft particle multiplicity. Consequently, the scaling employed is likely to somewhat underpredict the charm production in high multiplicity heavy ion collisions. Should pion annihilation be significant in nucleus-nucleus collisions, which seems likely with the large number of pions created, then care must be taken in scaling the expected annihilation rate. This should vary as the square of the charged particle multiplicity. As the data are very new, these quantitative studies are underway and we do not yet know how much of the observed enhancements can be explained without invoking new physics.

Returning to the ϕ, it should be noted that E859 has measured the $\phi \rightarrow K^+K^-$ decays in 14.6 GeV/nucleon Si+Au collisions.[51] They find that the ϕ mass and width are not modified and that the production rate is consistent with the measured charged kaon cross sections.

A feature visible in Figure 6 is the suppression of J/ψ production in S-W compared to p-W collisions. This suppression was reported to increase with increasing collision centrality already by NA38.[52,53] They also find that the ψ' is suppressed more strongly than the J/ψ.[50] It is necessary to take into account initial state parton scattering effects on $c\bar{c}$ production, and final state scattering of the J/ψ with the comoving hadrons before the observed suppression can be interpreted as a signal of new physics.[45] These effects can be quantified from p-nucleus data, where a suppression of J/ψ formation was observed for heavy targets.[54, 53] Initial state scattering broadens the parton p_t distribution; this p_t kick may increase with larger q^2 and decrease with larger $\sqrt{s}$. The final state J/ψ can also be dissociated by nuclear absorption or secondary scattering. In fact, p-nucleus and nucleus-nucleus collisions show a similar rate of J/ψ as a function of the number of nucleon-nucleon collisions. Fitting the magnitude of the initial and final state scattering effects from p-nucleus collisions, and comparing the result to observed J/ψ production in nucleus-nucleus, does not leave much room for new physics (but does not rule it out conclusively either).[55]

Direct photons can yield complementary and analogous information to thermal dileptons. Soft photons arise primarily from π^0 and η decays, but also have a contribution from the hot expanding hadron gas, which we wish to characterize. At high p_t (> 4-

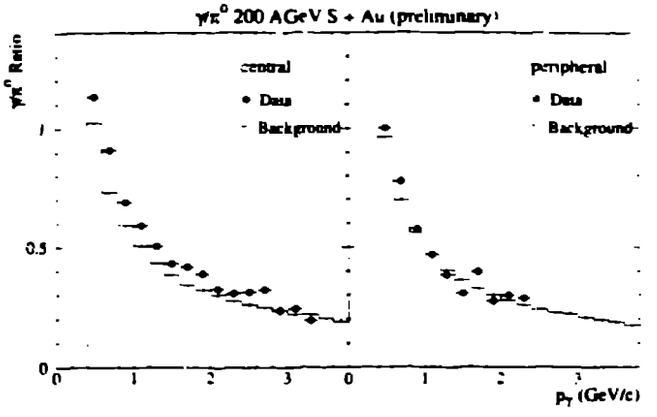

Figure 7. γ/π^0 ratio as a function of p_t for peripheral and central S + Au collisions at 200 GeV/nucleon, measured by WA80. The histograms indicate photons from hadronic sources.

5 GeV/c), the photon spectrum is dominated by parton annihilation if a quark-gluon plasma is formed. In measuring photons, the problem is to reconstruct π^0 and η distributions to quantitatively understand the dominant source of photons in the collisions. WA80 has searched for direct photon production by measuring the total photon distribution and comparing it to the π^0 yield.[56] Figure 7 shows the p_t dependence of the γ/π^0 ratio in peripheral and central S + Au collisions at 200 GeV/nucleon. The points show the data, and the histograms the "background" from hadron decays. It is evident that the peripheral collisions show no enhancement over background, but central collisions have an indication for direct photon production below $p_t \approx 2$ - 3 GeV/c.[56]

6. FUTURE

The immediate future in heavy ion collisions is the availability of 160 GeV/nucleon lead beams expected at CERN in November 1994. The major experiments are eagerly awaiting this opportunity to prepare even higher energy density systems in the laboratory. Further in the future are two heavy ion colliders: RHIC with $\sqrt{s} = 200$ GeV, under construction at Brookhaven, and the LHC at $\sqrt{s} = 5.5$ TeV, planned at CERN. RHIC will have two large experiments, PHENIX and STAR, focussing on lepton, photon and few-hadron measurements, and event-by-event hadron studies, respectively. There will also be two small experiments - PHOBOS and BRAHMS. Together these experiments will cover the range of observables. At the LHC there will be one very large heavy ion experiment, ALICE.

Figure 8 shows a prediction of contributions to the dilepton mass distribution in the high $\sqrt{s}$ collisions

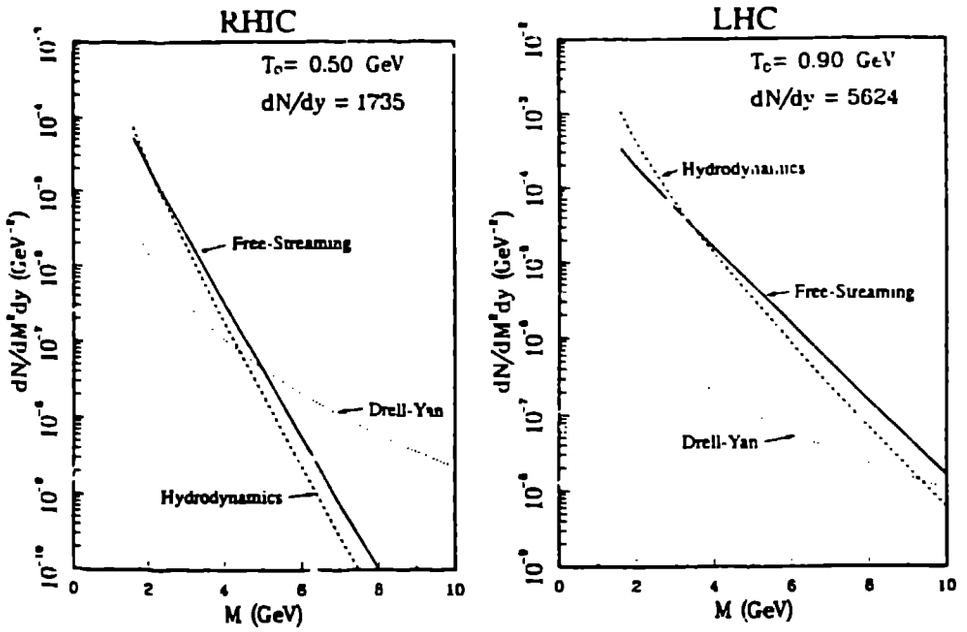

Figure 8. Dilepton mass distribution in free-streaming and hydrodynamic expansion calculations for heavy ion colliders. These are compared with the Drell-Yan contribution.

expected in the heavy ion colliders being built.[57] At the RHIC Collider the particle rapidity density (including neutral hadrons), dN/dy, expected is 1735. At the LHC, dN/dy will be 5624. These yield initial temperatures of 500 and 900 MeV, respectively, which will result in a much larger production of thermal dileptons at high mass than in current experiments. This is encouraging to experiment design as the thermal dileptons will be accessible away from the ρ, ω, ϕ and the complicated region below. Of course, the charged particle multiplicities are daunting. The solid and dashed lines on the figure show thermal dilepton mass distributions for both colliders with a calculation incorporating free streaming of particles longitudinally, and the standard Bjorken boost invariant hydrodynamical expansion, respectively. The dotted line is the standard estimate of the Drell-Yan yields (without the K factor). At RHIC, the thermal spectrum is above Drell-Yan to perhaps 4 or 5 GeV dilepton mass, and at LHC to 9 or 10 GeV.

7. CONCLUSIONS

The recent results highlighted at the conference and in this review show that we can study the dynamics of nucleus-nucleus collisions experimentally by measuring the correlations of hadron pairs. These measurements provide information about the evolution of the energy density in these complex systems. There is an enhancement in strangeness production in central nucleus-nucleus collisions which cannot be easily explained with known processes. Dileptons show excess production in high multiplicity nucleus-nucleus collisions in the soft (below the ρ) and intermediate (between the ϕ and J/ψ) continuum regions, and photons also show an enhancement over hadronic sources. The community is workingto understand these phenomena and is looking forward to the near future which will allow creation of high energy density matter over larger volume. The next 5-10 years will bring much larger $\sqrt{s}$, energy densities, and hopefully initial temperatures.

Acknowledgments

I would like to thank the heavy ion experiment collaborations for making their unpublished data available for this review, and for many discussions about the results. This work was supported by the U.S. Department of Energy under contract KB-02-01-00-0.

References

[1] T.D. Lee, Rev. Mod. Phys. **47** (1975) 267; G. Chapline and M. Nauenberg, Phys. Rev. **D16** (1977) 450.
[2] F. Karsch, Proc. of the NATO School on Particle Production in Highly Excited Matter, Il Ciocco, Italy, July 1992, p.207.
[3] F. Wilczek, Nucl. Phys. **A566** (1994) 123c.
[4] K. Rajagopal and F. Wilczek, Nucl. Phys. **B399** (1993) 395; **B404** (1993) 577.

[5] S. Pratt, Phys. Rev. **D33** (1986) 1314; G. Bertsch and G.E. Brown, Phys. Rev. **C40** (1989) 1830.
[6] K.S. Lee, U. Heinz, and E. Schnedermann, Z. Phys **C48** (1990) 525.
[7] R. D. Pisarski and F. Wilczek, Phys. Rev. **D29** (1984) 338.
[8] R.D. Pisarski, Phys. Lett. **B110** (1982) 155.
[9] M. Asakawa and C.M. Ko, Nucl. Phys. **A560** (1993) 399.
[10] D. Lissauer and E. V. Shuryak, Phys. Lett. **B253** (1991) 15.
[11] T. Matsui and H. Satz, Phys. Lett. **B178** (1986) 416
[12] R. Hagedorn and J. Rafelski, Phys. Lett. **B97** (1980) 180; J. Rafelski and B. Mueller, Phys. Rev. Lett. **48** (1982) 1066; P. Koch, B. Mueller and J. Rafelski, Phys. Rep. **142** (1986) 167.
[13] U. Heinz, P R. Subramanian and W. Greiner, Z. Phys. **A318** (1984) 247; P. Koch, B. Mueller, H. Stoecker and W. Greiner, Mod. Phys. Lett. **A3** (1988) 737.
[14] M. Gyulassy, Nucl. Phys. **A400** (1983) 31c; L. Van Hove, Z. Phys. **C27** (1985) 135.
[15] M. Gyulassy and M. Pluemer, Phys. Lett. **B243** (1990) 432; X.N. Wang and M. Gyulassy, Phys. Rev. Lett. **68** (1992) 1480.
[16] A. Shor, Phys. Lett. **B215** (1988) 375; **233B** (1989) 231.
[17] S. Pratt, T. Csorgo and J. Zimanyi, Phys. Rev. **C42** (1990) 2646.
[18] J. Sullivan, et al. Phys. Rev. Lett. **70** (1993) 3000.
[19] H. Beker, et al.(NA44 Collaboration), CERN-PPE/94-75, Z. Phys. in press.
[20] H. Beker, et al.(NA44 Collaboration), CERN-PPE/94-119, (1994).
[21] Th. Alber, et al.(NA35 Collaboration), IKF-HENPG/9-94 (1994).
[22] Th. Alber, et al.(NA35 Collaboration), submitted to Phys. Rev. Lett. (1994).
[23] T. Abbott, et al.(E802 Collaboration), Phys. Rev. Lett. **69** (1992) 1030.
[24] Y. Akiba, et al.(E802 Collaboration), Phys. Rev. Lett. **70** (1993) 1057.
[25] V. Cianciolo, Ph.D. thesis, MIT (1994).
[26] J.D. Bjorken, Phys. Rev. **D27** (1983) 140.
[27] T. Csorgo and B. Lorstad, Univ. Lund preprint LUNFD6/9NFF1-7082 (1994).
[28] H. Sorge, H. Stoecker and W. Greiner, Ann. Phys. **192** (1989) 266.
[29] J. Barrette, et al. (E814 Collaboration), Phys. Lett. B, in press.
[30] W.A. Zajc, Proc. of the NATO School on Particle Production in Highly Excited Matter, Il Ciocco, Italy, July 1992, p.435.
[31] U. Heinz, Nucl. Phys. **A566**, 205c (1994).
[32] H.C. Eggers and J. Rafelski, Int. J. Mod. Phys. **A6** (1991) 1067.
[33] T. Abbott, et al. (E802 Collaboration), Phys. Rev. Lett. **64** (1990) 847.
[34] H. Sorge, et al., Phys. Lett. **B271** (1991) 37.
[35] T. Akesson, et al. (HELIOS Collaboration), Phys. Lett. **B296** (1992) 273.
[36] J. Bartke, et al. (NA35 Collaboration), Z. Phys. **C48** (1990) 191.
[37] E. Anderson, et al. (NA36 Collaboration), Phys. Lett. **B294** (1992) 127; E. Anderson, et al. (NA36 Collaboration), Nucl Phys. **A566** (1994) 217c.
[38] S. Abatzis, et al. (WA85 Collaboration), Phys. Lett. **B270** (1991) 123 .
[39] H. Sorge, M. Berenguer, H. Stoecker and W. Greiner, Phys. Lett. **B289** (1992) 6.
[40] S. Abatzis, et al. (WA94 Collaboration), these proceedings.
[41] T. Akesson, et al. (AFS Collaboration), Nucl. Phys. **B246** (1984) 1.
[42] J. Cleymans, K. Redlich and H. Satz, Z. Phys. **C52** (1991) 517.
[43] E.V. Shuryak, Phys. Lett. **B78** (1978) 150.
[44] E.V. Shuryak, Phys. Rev. Lett. **68** (1992) 3270.
[45] S. Gavin and R Vogt, Nucl Phys. **B345** (1990) 104.
[46] A. Chilingarov, et al Nucl. Phys. **B151** (1979) 29.
[47] T. Akesson, et al. (HELIOS collaboration), CERN-PPE/94-140 (1994).
[48] A. Drees, et al. (CERES Collaboration, Nucl. Phys. **A566** (1994) 87c; Th. Ullrich, et al. (CERES Collaboration), these proceedings.
[49] A. Mazzoni, et al. (HELIOS/3 collaboration), Nucl Phys. **A566** (1994) 95c; M. Masera, et al. (HELIOS/3 collaboration), these proceedings.
[50] M. C. Abreu, et al. (NA38 Collaboration), Nucl. Phys. **A566** (1994) 77c; C. Lourenco, Proc. of the 5th Conference on Intersections between Particle and Nuclear Physics, S. Petersburg, Fl. (1994).
[51] Y. Wang, et al. (E859 Collaboration), Nucl. Phys. **A566** (1994) 379c.
[52] C. Baglin, et al. (NA38 Collaboration), Phys. Lett. **255** (1991) 459.
[53] C. Baglin, et al. (NA38 Collaboration), Phys. Lett. **270** (1991) 105.
[54] D. Alde, et al., Phys. Rev. Lett. 66 (1991) 133.
[55] S. Gavin, Proc. of the 4th Conference on Intersections between Particle and Nuclear Physics, Tucson, Az. (1991), p.879.
[56] R. Santo, et al. (WA80 Collaboration), Nucl. Phys.**A566** (1994) 61c.
[57] J. Kapusta, L. McLerran and D.K. Srivastava, Phys. Lett. **B283** (1992) 145.

B.F.L. Ward, Tennessee:
Could you tell us the strongest experimental evidence which you have that one has actually reached thermal equilibrium in the heavy-ion collisions?

Jacak:
We have not yet shown this unambiguously, but the single hadron distributions and correlation functions indicate a great deal of secondary scattering before freeze-out. The measured hadron transverse mass distributions approach m_t scaling, which would be expected in a thermalized system. Furthermore, the relative production ratios of different hadrons approach the values expected for chemical equilibrium.

A. Efremov, Dubna
There exists one more signal of the plasma. It is the decrease of strange baryon polarization. Does somebody try to observe this?

Jacak:
A search for Λ polarization was performed by NA35 and reported in reference 36. They found in S+S collisions no transverse or longitudinal polarization of the Λ, however the measurement is at the limit of statistical significance. It is important, however, to recall the large amount of secondary scattering undergone by the hadrons before they decouple; this limits the usefulness of polarization as a plasma signal.